PARTICLE ACCELERATION BY MAGNETIC RECONNECTION AND FAST MAGNETOSONIC SHOCK WAVES IN SOLAR FLARES

Jun-ichi Sakai* and Yukiharu Ohsawa**

ABSTRACT

This article reviews recent development of the theory of current loop coalescence and fast magnetosonic shock waves, giving particular attention to particle acceleration caused by these processes.

It is shown that the spiral, two sided plasma jets can be explosively driven by the plasma rotational motion induced by magnetic reconnection during the two current loop coalescence. The rebound following the plasma pinch driven by the Lorentz force can generate the fast magnetosonic shock waves.

For a weak magnetic field $(\omega_{ce} \ll \omega_{pe})$, strong acceleration by the shocks occurs to proton only. While the simultaneous acceleration of protons and electrons takes place in a rather strong magnetic field such that $\omega_{ce} \gtrsim \omega_{pe}$. Resonant protons gain relativistic energies within the order of the ion cyclotron period (much less than 1 s for solar plasma parameters). The electron acceleration time is shorter than the ion cyclotron period.

Keyword; Magnetic reconnection, Shock acceleration, plasma jet formation, Magnetic collapse, Solar flares, Current loop coalescence.

1. INTRODUCTION

The solar flare (for previous summaries, see Svestka[1], 1976; Sturrock[2], 1980; Kundu et al.[3], 1986; Sturrock et al.[4], 1986) is a manifestation of the explosive release process of magnetic energy stored in the lower corona. During the solar flare a large amount of energy, up to 10^{32} ergs, is released in the solar atmosphere with a time period of a few to about ten minutes. Energy release in solar flares can occur in various forms; plasma heating from 10^6 K to $5 \cdot 10^7$ K, acceleration of charged particles up to relativistic energy, plasma jet motions, and production of electromagnetic radiations in the range from the radio to γ-ray wavelengths.
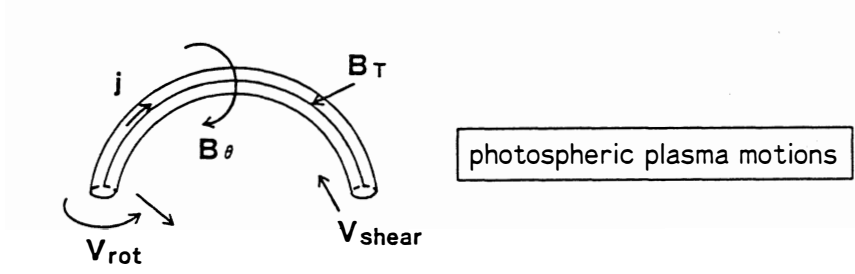
In order to fully understand the whole picture of solar flares, we must investigate at least the three physical processes related to magnetic energy, i.e., generation, storage, and dissipation of

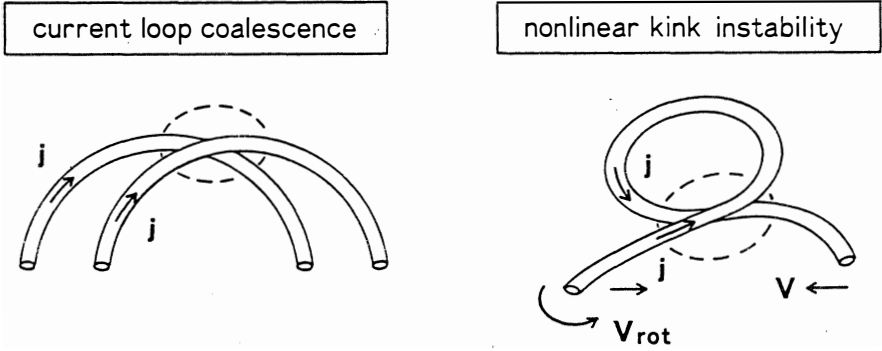* Department of Applied Mathematics and Physics, Faculty of Engineering,Toyama University, Toyama 930 Japan
** Institute of Plasma Physics, Nagoya University, Nagoya 464 Japan

Evolution of a Solar Flare

Current generation and storage of magnetic energy

j

B_T

B_θ

photospheric plasma motions

V_{rot}

V_{shear}

Dissipation of magnetic energy through reconnection

current loop coalescence

nonlinear kink instability

j

j

j

j

V_{rot}

V

Flare phenomena

plasma heating and plasma motions $\longrightarrow$ shock waves

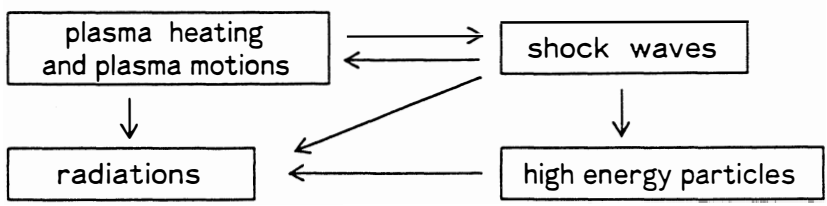radiations $\longleftarrow$ high energy particles

Fig.1 Evolution of a Solar Flare

magnetic energy. We show a possible senario for the solar flares in Fig.1 (Sakai and Ohsawa,[5] 1987), which has been drawn with particular attention to the generation, storage, and dissipation of magnetic energy.

Direct observations of soft X-rays (Howard and Svestka,[6] 1977) showed that multiple bright coronal loops exist in the magnetic active regions of many magnetic bipoles. These loops may carry plasma currents, which can be generated by photospheric plasma motions in active regions such as

shear motions of sun spots and rotational motions. Mutual interactions of interconnecting coronal loops could be quite an important physical process for magnetic energy release in solar flares (Gold and Hoyle,[7] 1960; Tajima et al.,[8] 1982; Tajima et al.,[9] 1987). In fact, recent observations of H_α emmision, radio waves (Kundu,[10] 1982) and hard X-rays (Machsdo et al.,[11] 1988) suggest that the interactions of coronal loops in the impulsive phase lead to the solar flare.

In order to explain the rapid quasi-periodic acceleration of both ions and electrons observed in the June 7, 1980 flare, Tajima and Sakai (1985,[12] 1986[13]) and Tajima et al. (1982,[8] 1987[9]) showed that the most likely mechanism for the impulsive release of magnetic energy in solar flares is the current loop coalescence (for review, see Sakai and Ohsawa, 1987[5]). It has been shown by theory and simulation (Sakai and Tajima,[14] 1986, Tajima and Sakai,[15,16] 1989) that during the coalescence of two current loops, the magnetic reconnection can explosively transform the magnetic energy to kinetic energy, producing high energy particles and increasing plasma temperatures. The transformation can occur within the Alfvén transit time across the currnt loops, which is about 1 ～ 10 s for appropriate loop radii. Furthermore, the energy release can be achieved in quasi-periodic manner, when the ratio B_p/B_t between the poloidal (B_p: produced by the loop current) and the toroidal (B_t: potential field) components of the magnetic field is greater than one. While in the reverse case. $B_p/B_t < 1$, the energy release by magnetic reconnection is not so explosive compared with the case of $B_p/B_t > 1$. In this situation the two current loops begin to rotate around the reconnection point shown in Fig.2 (Sakai,[17] 1989). After the coalescence of two current loops, the single current loop can still do the plasma rotational motion as shown in Fig.2 b-d
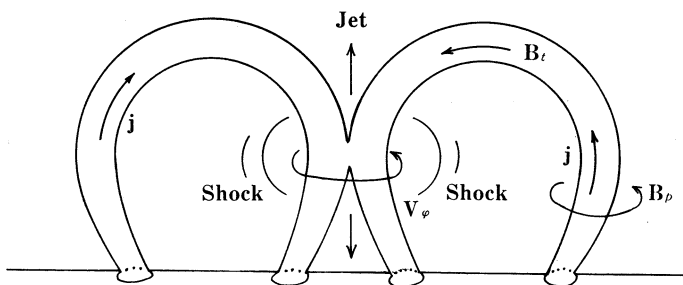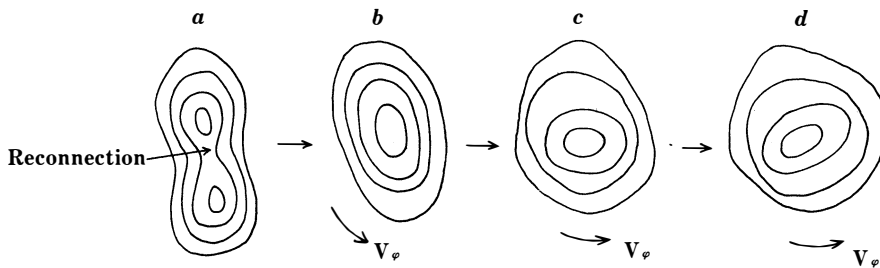
Loop-Loop Coalescence

Fig.2 Loop-Loop Coalescence

In section 2, we show the results of spiral plasma jet formation driven by the plasma rotational motion induced during the two current loop coalescence process (Sakai,[17] 1989). By means of a theoretical model based on the ideal MHD equations, we find that the spiral, two sided jets can be explosively produced by the combination of the magnetic pinch effect (magnetic collapse) and the plasma pressure. The plasma rebound flow following the magnetic collapse can strongly induce the super-Alfvénic plasma flow, which can generate the fast magnetosonic shock waves.

In section 3, as a possible mechanism for high energy particle acceleration in the impulsive phase of solar flares, a new particle acceleration mechanism in the fast magnetosonic shock waves is proposed (Ohsawa,[18] 1985; see for review, Sakai and Ohsawa,[5] 1987). The collisionless fast magnetosonic shocks can promptly accelerate protons and electrons to relativistic energies, which was found by theory and relativistic particle simulation (Ohsawa and Sakai,[19] 1987; 1988a,[20] 1988b[21]). The simultaneous acceleration of protons and electrons takes place in a rather strong magnetic field such that $\omega_{ce} \gtrsim \omega_{pe}$. Resonant protons gain relativistic energies within the order of the ion cyclotron period (much less than 1 s). The electron acceleration time is shorter than the ion cyclotron period.

In section 4, we discuss some applications to solar flares.

2. PLASMA JET AND SHOCK FORMATION DURING CURRENT LOOP COALESCENCE

The magnetic reconnection process during the current loop coalescence was reviewed by Sakai and Ohsawa (1987),[5] in which the effect of toroidal magnetic field (B_t) on reconnection was discussed. When the toroidal field, B_t is less than the poloidal field, B_p, explosive reconnection is observed and instead a plasma rotational motion around the reconnection point occurs when B_t becomes larger than B_p. This plasma rotational motion after the magnetic reconnection can be observed in the computer simulation of the two current loop coalescence (Zaidman,[22] 1986). We call this the threshold phenomena with the toroidal magnetic field. The same threshold phenomenon as the above is observed in simulations of reconnection triggered by impinging MHD waves (Sakai et al.[23] 1984).

We consider the single current loop which can be produced by the two current loop coalescence shown in Fig.2. After the magnetic reconnection, the single current loop can be produced and the plasma can be heated by the magnetic energy dissipation. At the same time, the plasma rotaional motion (V_ϕ) around the reconnection point can be induced during the loop coalescence process when the ratio B_p/B_t is less than one.

In order to represent the spiral plasma jet nd spiral magnetic field structure associated with the jet which may be generated during the above process, we assume the physical quantities as follows; for the velocity components,

$$\left. \begin{array}{l} V_r = \dfrac{\dot{a}}{a}r, \\[2mm] V_\phi = \dfrac{\dot{c_1}}{c_1}r, \\[2mm] V_z = \dfrac{\dot{b}}{b}z, \end{array} \right\} \tag{2.1}$$

for magnetic field components,

$$
\left.
\begin{aligned}
B_r &= \frac{B_{10}}{a^2 b}\left(\frac{r}{\lambda}\right), \\[4pt]
B_\phi &= \frac{B_{20}}{a^2 b}\left(\frac{r}{\lambda}\right), \\[4pt]
B_z &= \frac{B_0}{a^2} - 2\frac{B_{10}}{a^2 b}\left(\frac{z}{\lambda}\right),
\end{aligned}
\right\}
\tag{2.2}
$$

where we used the cylindrical coordinates (r,ϕ,z), and the dot means the time-derivative. The time-dependent scale factors, $a(t)$, $c_1(t)$ and $b(t)$ can be self-consistently determined from the ideal MHD equations with the adiabatic law $(p \sim \rho^\gamma)$. B_{10}, B_{20} and B_0 are constants and λ is a characteristic scale length which we are concerned with. From the continity equation. we find the density ρ as $\rho = \rho_0/a^2 b$, where ρ_0 is a constant. From the Maxwell equation, we obtain the current $j_z = cB_{20}/2\pi\lambda a^2 b$, which flows along the loop. The time-dependent scale factors can be determined from the equations of motion as follows

$$
\frac{d^2 a}{dt^2} = \frac{c_s^2}{\lambda^2 a^{2\gamma-1} b^{\gamma-1}} - \frac{2v_A^2}{\lambda^2 ab} + a\left(\frac{\dot{c_1}}{c_1}\right)^2,
\tag{2.3}
$$

$$
\frac{d^2 b}{dt^2} = \frac{c_s^2}{\lambda^2 a^{2\gamma-2} b^\gamma},
\tag{2.4}
$$

$$
\frac{d^2 c_1}{dt^2} = \frac{2v_{A2}^2 c_1}{\lambda^2 a^2 b} + \frac{\dot{c_1}^2}{c_1} - 2\frac{\dot{a}}{a}\dot{c_1}^2,
\tag{2.5}
$$

where $c_s^2 = p_{10}/\rho_0$, $v_A^2 = B_{20}^2/4\pi\rho_0$, $v_A^2 = v_A(B_{10}/B_{20})^{1/2}$.

We here assume that the pressure is given by

$$
p(r,z,t) = p_0(t) - \frac{(p_{1r}(t)r^2 + p_{1z}(t)z^2)}{2\lambda^2},
\tag{2.6}
$$

where $p_0(t), p_{1r}(t)$ and $p_{1z}(t)$ can be determied from the adiabatic law as

$$
\left.
\begin{aligned}
p_0(t) &= p_{00}/(a^2 b)^\gamma, \\[4pt]
p_{1r}(t) &= p_{10}/(a^{2(\gamma+1)} b^\gamma), \\[4pt]
p_{1z}(t) &= p_{10}/(a^{2\gamma} b^{\gamma+2}),
\end{aligned}
\right\}
\tag{2.7}
$$

where p_{00} and p_{10} are constants.

We show numerical results obtained from Eqs. (2.3) − (2.5), which determine the all physical quantities such as the velocity field (2.1) and the magnetic field (2.2). The time is normalized by the Alfvén transit time $\tau_A = \lambda/v_A$. The velocity is normalized by the Alfvén velocity which is determined from the poloidal magnetic field B_{20}. The initial conditions for the velocities are $v_r = -10^{-6}(v_A r/\lambda)$, $v_z = 10^{-6}(v_A z/\lambda)$ and $v_\phi = 0.1 (v_A r/\lambda)$. The plasma beta ratio is taken to be 0.01.
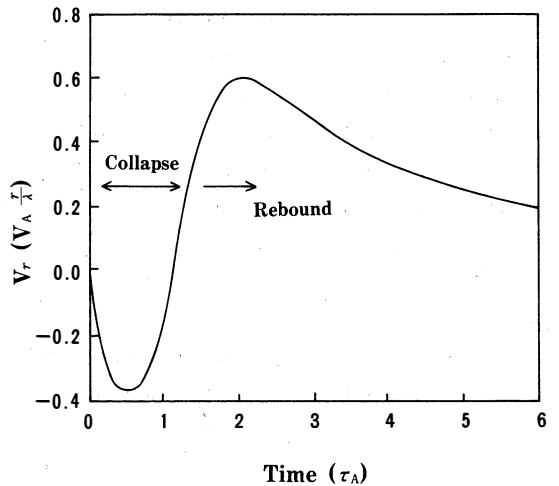

Fig.3

We take $B_1 = B_0$ and $\gamma = 5/3$. Figure 3 shows the time evolution of the radial plasma flow velocity.

The initial rotational plasma flow induced after the magnetic reconnection can drive the plasma collapse $(v_r < 0)$ mainly by the $j_z \times B_\phi$ force, which corresponds to the second term of the right-hand side of Eq. (2.3). During the plasma collapse, the explosive plasma jet in the z-direction can be produced as seen in Fig.4. The acceleration time to the maximum velocity of the jet is quite short and about 0.11 τ_A. The plasma jet can be driven by the combination of two forces. namely, the $j_z \times B_\phi$ (which drives the magnetic collapse) and the pressure gradient $\partial p / \partial z$. The jet maximum velocity obtained during the short time period is not so sensitive to the initial rotational velocity. We found the same results for the cases $V_\phi = 0.01 - 1 (v_A r / \lambda)$. The most important parameter which determines the maximum jet velocity and the acceleration time is the plasma beta ratio. When the beta ratio decreases, the maximum jet velocity also decreases and the acceleration time becomes long. While the beta ratio increases. the maximum jet velocity increases and becomes super-Alfvénic within the very short time period.

The plasma jet obtained here shows the two sided flows which originate from the current coalescence region as seen in Fig.2.

Fig.4

Fig.5

As seen in Fig.3, the plasma rebound $(v_r > 0)$ can occur following the plasma collapse. The velocity of the rebound can be enhanced by the magnetic collapse and adiabatic compression, when the plasma beta ratio is small. We here investigate the condition of fast magnetosonic shock waves by the rebound after the magnetic collapse. In the low beta plasma , the shock formation condition, $v_r > (v_A^2 + c_s^2)^{1/2}$, is given by

$$\left[\dot{a}^2 - \frac{1}{b} \left\{ 1 + \left(\frac{B_{10}}{B_{20}} \right)^2 \right\} \right] \left(\frac{r}{\lambda} \right)^2 > b \left(\frac{B_0}{B_{20}} \right)^2. \qquad (2.8)$$

We obtain one condition which must be satisfied in Eq. (2.8). Namely, the term with a parenthesis of the left-handed side must be positive,

$$\sqrt{b} \, \dot{a} > \left\{ 1 + \left(\frac{B_{10}}{B_{20}} \right)^2 \right\}^{1/2}. \qquad (2.9)$$

If the condition (2.9) is satisfied, the fast magnetosonic shock wave can be generated in the region of $r > r_s$, where r_s is given by
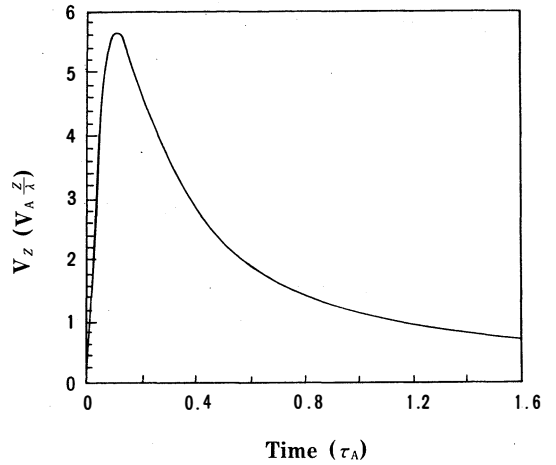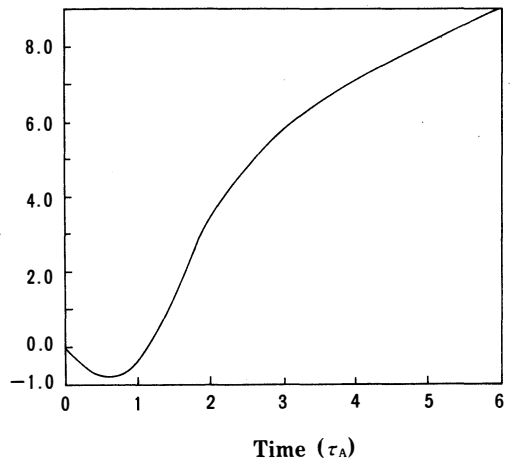
$$\sqrt{r_s} = \sqrt{b}\left(\frac{B_0}{B_{20}}\right)\left[\dot{a}^2 - \frac{1}{b}\left\{1 + \left(\frac{B_{10}}{B_0}\right)^2\right\}\right]^{-1/2}\lambda. \qquad (2.10)$$

Figure 5 shows the time variation of $\sqrt{b}\,\dot{a}$ in the case of $B_{10} = B_{20} = -1$. The region where $\sqrt{b}\,\dot{a} > \sqrt{2}$ is satisfied can be observed in Fig.5. The radius where the shock can be produced is around the scale length λ.

If we take $\lambda \sim 10^8$cm which corresponds to the loop radius, and the Alfvén velocity $v_A \simeq 500$km/s, the Alfvén transit time is $\tau_A = \lambda/v_A = 2$seconds. Therefore the acceleration time to the maximum jet velocity is $0.1 \sim 1$s, depending on the plasma beta ratio.

The two sided jet flows originated from the current loop coalescence region may be observed during the impulsive phase.

During the plasma collapse, the strong electric field, $\mathbf{E} = -(\mathbf{V} \times \mathbf{B})/c$ can be produced by the change of the magnetic field. This electric field can generate high energy particles within one second.

3. PROMPT SIMULTANEOUS ACCELERATION OF PROTONS
AND ELECTRONS TO RELATIVISTIC ENERGIES BY SHOCK WAVES

In previous section we showed that the fast mode shocks by the rebound following the magnetic collapse is very effectively formed, even though the colliding velocity of the two current loops is much less than the Alfvén velocity.

Recently theoretical and simulation work (Ohsawa et al.[18-21]) has shown that a quasi-perpendicular fast magnetosonic shock wave can accelerate both protons and electrons to relativistic energies within a very short time period (shorter than 1 s for the solar plasma parameters). The simultaneous acceleration takes place in a rather strong magnetic field $(\omega_{ce} \gtrsim \omega_{pe})$. For weak magnetic field $(\omega_{ce} \ll \omega_{pe})$, strong acceleration occurs to protons only.

When the ambient magnetic field is weak $(\omega_{ce} \ll \omega_{pe})$, fast magnetosonic shock waves are well described by nonrelativistic theory (Adlam and Allen[24],1958; Davis et al.[25],1958; Sagdeev[26],1966). For such nonrelativistic shocks, it is known (Ohsawa[18],1985; Ohsawa and Sakai[19],1987) that a quasi-perpendicular fast magnetosonic shock wave can trap some ions and resonantly accelerate time in the direction perpendicular to the ambient magnetic field and parallel to the wave front up to the speed

$$v \sim v_A \left(\frac{m_i}{m_e}\right)^{1/2}(M-1)^{2/3}, \qquad (3.1)$$

where M is the Alfvén Mach number. Those trapped ions are accelerated within a short time period, $t \sim \omega_{ci}^{-1}(m_i/m_e)^{1/2}$, where ω_{ci}. is the ion cyclotron frequency. When the resonant ions reach the maximum speed, equation (3.1), they are etrapped and left behind the shock front. For simplicity, we have written the expression of the maximum speed for a perpendicular shock in a zero beta plasma (for the maximum velocity in oblique shocks in finite beta plasmas, see Ohsawa, 1986[27], 1986[28]).

Equation (3.1) indicates that the maximum speed of resonantly accelerated ions increases with the Alfvén speed. Further it suggests that the resonant ions gain relativistic energies when the Alfvén speed is rather large, $v_A > c(m_e/m_i)^{1/2}$; this is equivalent to the condition $\omega_{ce} \gtrsim \omega_{pe}$. We will

discuss shock waves and particle acceleration in such a parameter regime.

First, we analytically show very briefly that ions can be promptly accelerated to relativistic energies for a rather strong magnetic field $\omega_{ce} \gtrsim \omega_{pe}$. From the analysis of single particle orbits in a monochromattc electrostatic wave $E = E_x \sin(kx - \omega t)$ propagating across the magnetic field B that points in the z-direction, it was shown (Sagdeev and Shapiro 1973[29] Sugihara and Midzno,1979)[30] that trapped particles can be accelerated in the direction parallel to the wave front and perpendicular to the magnetic field up to the speed $v \sim cE_x/B$. The strong longitudinal electric field in the shock region also traps some ions and resonantly accelerates them by the same mechanism. The quantity cE_x/B in a shock wave can be calulated from the self-consistent nonlinear wave theory, and the maximum speed of resonantly accelerated ions is found to be

$$V_{max} \sim c(1 - Q^{-2})^{1/2}, \tag{3.2}$$

where

$$Q = 1 + \frac{\omega_{ce}^2}{2\omega_{pe}^2}(\tilde{B} - 1)^2 \left[1 - \frac{(\tilde{B} + 1)^2}{(\tilde{B}_m + 1)^2}\right], \tag{3.3}$$

with $\tilde{B}$ the magnetic field strength normalized to the far upstream magnetic field strength B_0, $\tilde{B} = B/B_0$, and $\tilde{B}_m$ is the maximum value of $\tilde{B}$. When the ambient magnetic field is weak, Eq. (3.2) reduces the nonrelativistic equation (3.1). The resonant ions gain relativistic energies in the time period $t \sim \omega_{ci}^{-1}(m_i/m_e)^{1/2}$.

Next, we show simulation results; a relativistic particle simulation demonstrates a shock wave does accelerate some ions to relativistic energies, if the ambient magnetic field is rather strong($\omega_{ce} \gtrsim \omega_{pe}$). Moreover, some electrons are also accelerated to relativistic energies; this is in contrast to the nonrelativistic shocks in weak magnetic fields ($\omega_{ce} \ll \omega_{pe}$), in which strong acceleration occurs to ions only.

To study time evolution of shock waves, we use a $1 - 2/2$ dimension (one dimension in real space and three dimension in velocity space), fully relativistic, fully electromagnetic particle simulation with full ion and electron dynamics (for details of the code, see Ohsawa,1985)[18]. In this particle code, each simulation particle moves according to the relativistic equation of motion. The electric and magnetic fields are governed by full Maxwell equations. The total number of simulation particles is $N_i = N_e = 65000$. The total grid size is $L_x = 1024\Delta_g$, where Δ_g is the grid spacing. All length and velocities in our simulations are normalized to Δ_g and $\omega_{pe}\Delta_g$, respectively.

The simulation parameters are the following. The ion-to-electron mass ratio is $m_i/m_e = 100$. The speed of light is $c = 4$. In the upstream region, the ion temperature is equal to the electron temperature $T_i = T_e$, With the ion thermal speed $v_{Ti} = 0.081$ and the electron thermal speed $v_{Te} = 0.81$. The strength of the external magnetic field is chosen so that $\omega_{ce}/\omega_{pe} = 3$ in the far upstream
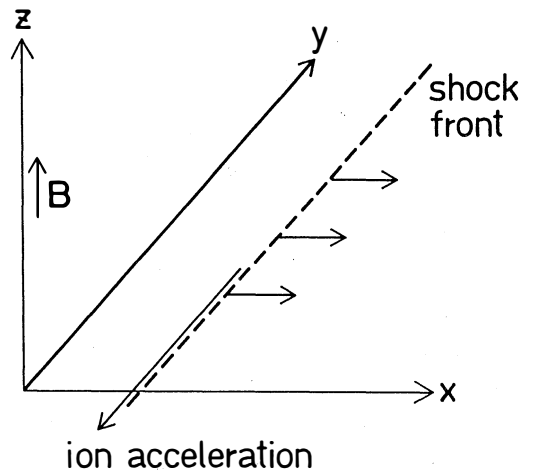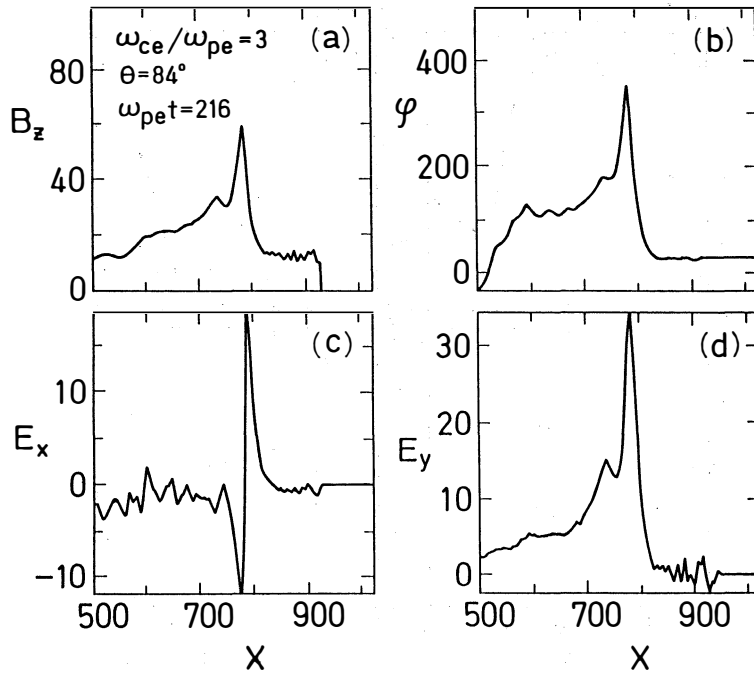

ion acceleration

Fig.6

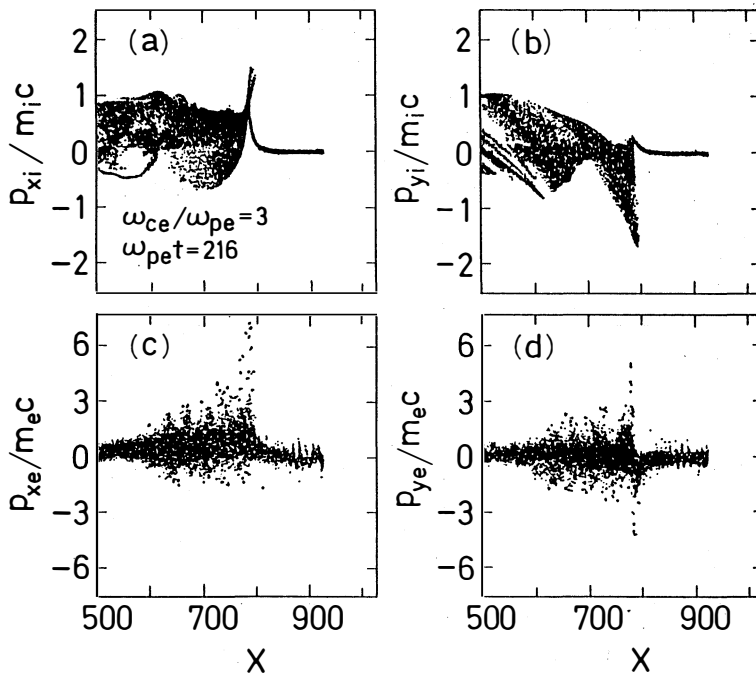Fig.7 Shock profile and the shock front is $x \simeq 800$.

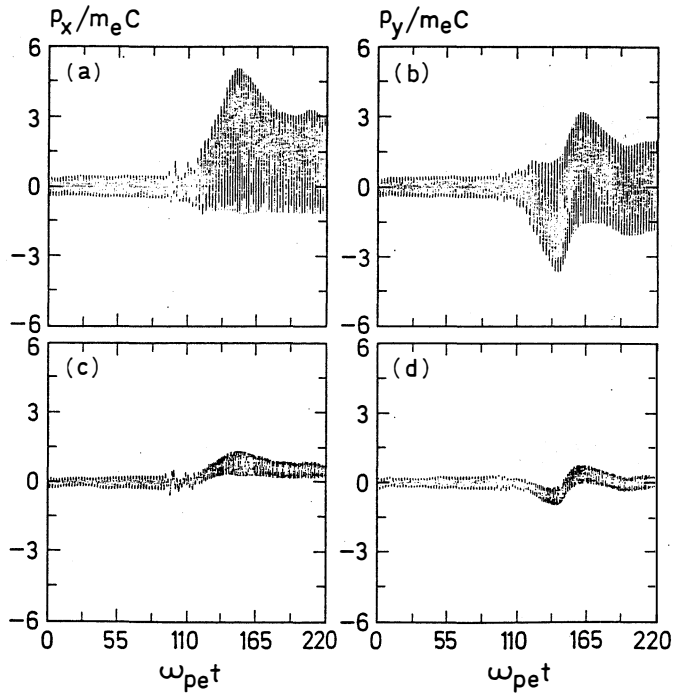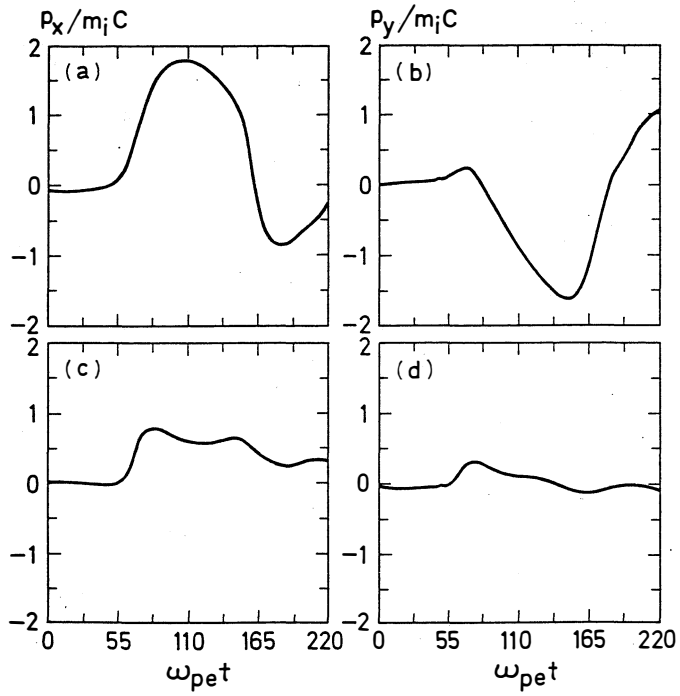Fig.8 Phase-space plots of ions(a) & (b) of electrons (c) & (d)

Fig.9 Time variations of momenta of strongly accelerated ion (a) & (b) and electron (c) & (d).

region. For these parameters, the Alfven speed is $v_A = 1.2$; the ion Larmor radius is 2.8; the electron inertial length is $c/\omega_{pe} = 4$. The plasma beta ratio in the far upstream is $\beta = 0.02$.

Figure 6 shows the coordinate system, in which the shock front and the direction of accelerated ion are shown. Figure 7 shows shock profile at $\omega_{pe}t = 216$. (a) is the magnetic field $B_z(x)$, (b) the potential ϕ, (c) the longitudinal electric field $E_x(x)$, and (d) the transverse electric field E_y. The propagation angle of the is 84°. The shock is propagating in the positive x-direction with Alfvén Mach number $M = 2.3$, and the shock front is at $x \simeq 800$ at $\omega_{pe}t = 216$. It is to be noted that in a relativistic shock wave the electric fields are so strong that the quantities E_x/B_z and E_y/B_z are of the order of unity in the shock region, while in nonrelativistic shocks those quantities are much smaller than unity.

Fig.10

Figure 8 shows phase-space plots of ions [(a) & (b)] and of electrons [(c) & (d)]. Both ions and electrons are strongly accelerated in the shock region to relativistic energies.

The acceleration mechanism of electrons is different from that of ions. It can be easily seen from Figure 9 which shows typical time evolution of the momenta of a strongly accelerated ion [(a) & (b)] and of an electron [(c) & (d)]. Figures 9(a) & (b) show that a trapped ion is accelerated in the direction of the wave normal and to the negative y-direction until it is detrapped. While the electron gains kinetic energy making Larmor gyration many times as seen in Fig.9(c) & (d). The electron acceleration time is about the transit time of the plasma across the shock region ($t \sim \Delta/v_{sh}$ with Δ the shock width and v_{sh} the shock speed) andhence much shorter than the ion cyclotron period.

Figure 10 shows the electron ditribution function in the region $640 \leq x \leq 800$. Up to now, we do not have a theory that predicts the precise shape of the energy distribution function.

4. DISCUSSION

We have shown from a simple theoretical model based on the ideal MHD equations that the two sided plasma jets can be explosively produced within the short time period. The fast magnetosonic shock waves can also be generated from the rebound after the plasma collapse. The fast magnetosonic shock waves can promptly accelerate both electrons and ions to relativistic energies. This mechanism could play an essential role in the particle acceleration in the impulsive phase of solar flares. It explains following important features: (1) the acceleration occurs simultaneously to protons and electrons, (2) the acceleration time is quite rapid (within 1s), and (3)protons and electrons are accelerated to relativistic energies. If shock waves produced in rather strong magnetic field region where the current loop coalecence occurs ($B_t > B_p$) propagate out to weak magnetic field regions, they will become ineffcient in accelerating electrons. However, they will continue to produce high energy protons, as in the 1982 June 3 solar flare(Forrest et al.[3]1987).
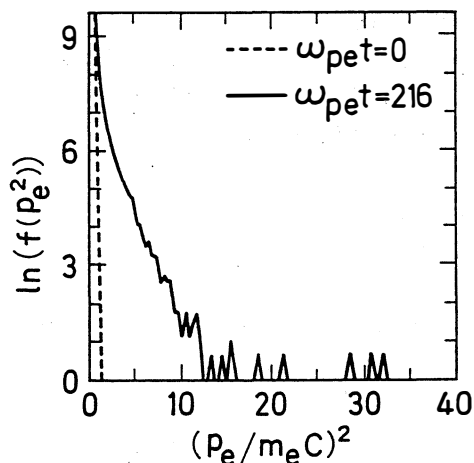
REFERENCES

1. Svestka, Z.: 1976, *Solar flares*, D.Reidel Publ.Co.,

2. Sturrock, P.A. (ed.): 1980, *Solar Flares*: *Monograph from Skylab Solar Workshop II*, Colorado Associated University press.

3. Kundu, M.R. and Woodgate. B. (eds.): 1986, *Energetic Phenomena on the Sun*, NASA Conf. Publ. No.2439.

4. Sturrock, P.A. et al. (eds); 1986, *Physics of the Sun*, D.Reidel Publ., Co., Dordrecht, Holland.

5. Sakai, J-I., and Ohsawa, Y.: 1987, *Space Sci. Rev.*, 46, 113.

6. Howward, R.,and Svestka, Z.: 1977, *Solar Phys.*, 54, 65.

7. Gold, T. and Hoyle, F.: 1960, *M.N.R.A.S.*, 120, 89.

8. Tajima, T. Brunel, F. and Sakai, J-I.: 1982, *ApJ.*, 245, L45.

9. Tajima, T., Sakai, J-I., Nakajima, H., Kosugi, T., Brunel, F. and Kundu, M.R.: 1987, *ApJ.*, 321, 1031.

10. Kundu, M.R.: 1982, *Rep. Prong. Phys.*, 45, 1435.

11. Machado, M.et al.: 1988, *ApJ.*, 326, 425.

12. Tajima, T., and Sakai, J-I.: 1985,IFSR No.197, Institute for Fusion Studies, Univ. of Texas.

13. Tajima, T., and Sakai, J-I.: 1986, *IEEE Tranc.*, *Plasma Sci.*, PS-14, 929.

14. Sakai, J-I., and Tajima, T.: 1986,in *Proc. of the Joint Varenna-Abatumani Int. School and Workshop on Plasma Astrophysics*, ESA SP-251,p.77.

15. Tajima, T., and Sakai, J-I.: 1989, *Sov., J.Plasma Phys.* in press.

16. Tajima, T., and Sakai, J-I.: 1989,*Sov., J.Plasma Phys.* in press.

17. Sakai, J-I.: 1989, *Solar Phys.* in press.

18. Ohsawa, Y.: 1985, *Phys. Fluids*, 28, 2130.

19. Ohsawa, Y., and Sakai, J-I.: 1987,*Ap. J.* 313, 440.

20. Ohsawa, Y., and Sakai, J-I.: 1988,*Ap. J.* 332, 439.

21. Ohsawa, Y., and Sakai, J-I.: 1988, *Solar Phys.* 116, 157.

22. Zaidman, E.G.: 1986, IFSR No.246, Institute for Fusion Studies, Univ. of Texas.

23. Sakai, J-I., Tajima, T., and Brunel, F.: 1984, *Solar Phys.*, 91, 103.

24. Adlam, J.H., and Allen, J.E.: 1958, *Philos.*, *Mag*.3, 448.

25. Davis, L., Lust, R., and Suhluter, A.: 1958, *Z.Naturforsch.* A13, 916.

26. Sagdeev, R.Z.: 1966, *in Reviews of plasma Physics*, Vol.4 Consultants Bureau,New York, p.23-91.

27. Ohsawa, Y.: 1986, *Phys. Fluids*, 29, 773.

28. Ohsawa, Y.: 1986, *Phys. Fluids*, 29, 1844.

29. Sagdeev, R.Z., and Shapiro, V.D.: 1973, *JETP Letters*, 17, 279.

30. Sugihara, R., and Midzno, Y.: 1979, *J.Phys. Soc. Jpn.* 47, 1290.

31. Forrest, D.J., et al.: 1987, *Adu. Space Res.* in press.